Hovering Performance of Plenum Chamber GEMS over Land and Water

DAVID I. G. JONES*
Vickers-Armstrongs Ltd., Swindon, England

A simple theory is developed for the prediction of the hovering performance of a plenum chamber type of ground effect machine over land and water. The analysis should assist in the understanding of the performance of full scale craft over water. The theory shows that a single nondimensional parameter controls the phenomena associated with overwater operation, and the experimental results compare well with the theory. It has not been possible to establish theoretically that the same nondimensional parameter also controls the rate of spray generation, but it is shown that the experimental data support such a view.

Nomenclature

C_i = discharge coefficient for air entering cushion ($= m/V_i lt\rho$); ratio of actual mass flow to theoretical
C_e = discharge coefficient for air leaving cushion (overland) ($= m/Vlh\rho$)
C_{ew} = discharge coefficient for air leaving cushion (overwater) [$= m/Vl(h + \Delta h)\rho$]
cos = circular cosine function
cot = circular cotangent function
f = ratio of cushion pressure to total head p/H
h = hoverheight or hovergap, i.e., distance from rim of craft to ground or undisturbed water surface
H = total head of air supplied to inlet of cushion
J = momentum of air leaving cushion at outlet
l = width of two-dimensional plenum chamber
m = mass flow rate through system
M = mass of spray generated in unit time
p = cushion pressure
sin = circular sine function
t = thickness of inlet nozzle in two dimensional case
tan = circular tangent function
V = mean velocity of air escaping from cushion at outlet
V_i = theoretical mean velocity of air entering cushion ($m/\rho lt$)
w = weight per unit volume of water
x = vertical distance from horizontal z axis
z = horizontal distance in outward direction from point where momentum of escaping air first starts cutting depression in water (see Fig. 4)
Z = horizontal distance from origin of z to point at which escaping air leaves water surface (see Fig. 4)
γ = nondimensional mass flow parameter [$= m/lC_i t(\rho p)^{1/2}$]
Γ = nondimensional parameter controlling overwater performance [$\Gamma = p/8w\ C_i t\xi_w$]
Δz = small change in z
Δh = amount by which water surface is depressed near outlet by momentum of escaping air (see Fig. 4)
ξ = ratio of effective outlet area to effective inlet area [$= C_e h/C_i t$]
ξ_w = value of ξ applicable to overwater operation [$= C_{ew}(h + \Delta h)/C_i t$]
ρ = density of air
ϕ = angle escaping air makes with water surface outside cushion (see Fig. 4)

Subscripts

e = exit
i = inlet
w = overwater operation

Glossary of terms

cushion = volume of high pressure air supporting craft and maintained by air flow through inlet nozzle
GEM = ground effect machine
hoverheight (or hovergap) = height of gap under rim of plenum chamber through which air escapes to atmosphere
inlet = gap or nozzle through which air enters cushion
outlet = gap (or, effectively, orifice) through which air escapes from cushion to atmosphere
plenum chamber = type of GEM whereby air is forced into an inverted bowl type of container which then rises from the ground; the air escapes under the rim of the bowl to atmosphere

Introduction

THE plenum chamber is the simplest GEM concept known. At first sight its performance does not seem to measure up to that of, for example, the peripheral jet GEM, but Chaplin[1] shows that much of the performance discrepancy is likely to be made up in practice. At the time he had no experimental data to help him. The present report concerns a similar approach to overland performance, and comparison made with experimental data is encouraging.

The overwater performance of the GEM has not been predicted with anything like the same success, although the problem is discussed with reference to peripheral jet vehicles by Eames[2] and Poisson-Quinton.[3] The present analysis is simple in concept and not unduly complicated in practice. Its basis is simply the application of Newton's second law to the vertical and horizontal components of the forces arising because of the reaction between the water surface and the air escaping from the cushion. Experimental verification is encouraging although additional data on larger test facilities would be desirable. A nondimensional parameter Γ is shown to control all of the phenomena involved in the analysis, and it was surmised that it would make an interesting experiment to determine whether or not there exists a significant causal relationship between the rate of spray generation and this

Received October 21, 1965; revision received February 14, 1966. The author would like to thank Vickers-Armstrongs Ltd. for permission to publish this paper, and M. Blake, M. J. Bennison, and J. W. Leathers for their interest in the work. Also, thanks are due to C. Mantych for assistance with preparation of the manuscript and figures.

* Senior Aerodynamicist; presently Research Engineer, Air Force Materials Laboratory, Wright-Patterson Air Force Base, Ohio.

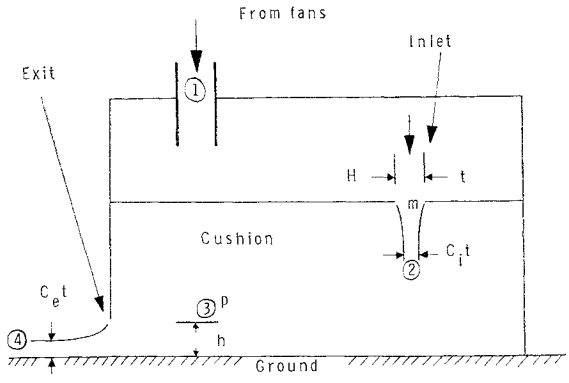

Fig. 1 Section of two-dimensional plenume hamber.

same parameter Γ. It was most obvious at the time the tests were being conducted that the spray generation rate was small when Γ was small, and large with Γ large. Available experimental data support this view.

Doubtless, more work on the overwater performance of GEMS of all types has been carried out in the last few years, but very little of this seems to have reached the literature as yet. It is to be hoped that the situation will be remedied in the future.

Theory of Overland Operation

The analysis presented herein is concerned only with two-dimensional phenomena, but the results may be carried over to simple three-dimensional craft without difficulty. High pressure air at total head H is delivered by a fan, or fans, to the vicinity of the inlet slot or nozzle. Discharge occurs through the inlet to the main air cushion at a static pressure p, and then finally discharges under the rim of the vehicle to atmospheric pressure. It is assumed that the coefficients of discharge are C_i and C_e at inlet and exit, respectively (see Fig. 1). The problem of insuring that the craft is in stable equilibrium is not discussed here, since it is assumed that this can be dealt with independently.

We now apply Bernoulli's equation to the flow out of the cushion to atmospheric pressure, i.e., from area three to area four in Fig. 1. Then, if the air from the inlet nozzle is assumed to diffuse completely before discharging to atmospheric pressure

$$\begin{aligned} 0 + (\rho/2)(m/\rho l C_e h)^2 &= p \\ m/lC_i t(\rho p)^{1/2} &= 2^{1/2}(C_e h/C_i t) = 2^{1/2}\,\xi \end{aligned} \tag{1}$$

where

$$\xi = C_e h/C_i t \tag{2}$$

A graph of $m/lC_i t(\rho p)^{1/2}$ vs ξ is shown in Fig. 2, and data obtained in the experimental phase of the investigation, to be described presently, also are shown. Apply Bernoulli's equation to the flow from area one to area two through the inlet slot as follows:

$$\left.\begin{aligned} p + (\rho/2)(m/\rho l C_i t)^2 &= H \\ H/p &= 1 + [m/lC_i t(\rho p)^{1/2}]^2/2 \\ &= 1 + \xi^2 \qquad \text{by Eq. (1)} \\ p/H &= (1 + \xi^2)^{-1} \end{aligned}\right\} \tag{3}$$

A graph of p/H vs ξ is shown in Fig. 3, along with experimental data. It is seen, therefore, that the parameter ξ controls the performance of the craft, and that ξ should be kept as low as possible in order for p/H to be as large as possible and the mass flow as small as possible. This means, according to Eq. (2), that, for given h and t, C_e should be as small as possible and C_i as large as possible. C_i can be made nearly 1.0 by carefully making the rim of the craft as thin and sharp as possible, i.e., effectively a sharp-edged orifice.

If the exit nozzle is aerodynamically "smooth", C_e will approach 1.0 and, in addition to that, the air from the inlet nozzle will be encouraged to flow easily, with much less than complete diffusion, through the cushion. Performance then will be reduced even further. Tests are described later which verify, to some extent, the results of this theory. Now it is of interest to apply a similar method of analysis to the craft over water.

Theory of Overwater Operation

Figure 4 shows the shape in which the water surface is assumed to deform. The main depression is caused by the cushion pressure p and is of depth p/w below the main water surface, where w is the weight per unit volume of water. The escaping air causes a further depression near the rim of the plenum chamber because of the momentum of the air. It is assumed that the static pressure of the air is atmospheric over the whole of the additionally deformed area. This implies that the escaping air contracts rapidly. No information concerning the shape of the deformed water surface has been found in the literature by the author. In the present series of tests, a few photographs were taken, and Fig. 5 represents the clearest of these. Although the violent motion of the water surface made photography difficult, the shape of the deformed water surface can be seen to be of the general form assumed in Fig. 4. At any rate, we shall allow this viewpoint to stand as a reasonable hypothesis.

Because the escaping air is forced to take a more restrained path than in the overland case, the outlet discharge coefficient C_{ew} for the overwater case will be lower than the corresponding coefficient C_e for the overland case. No certain knowledge is available, but it is probable that no matter what the value of C_e may be, C_{ew} will always be about 0.70. Certainly, it is difficult to produce discharge coefficients much

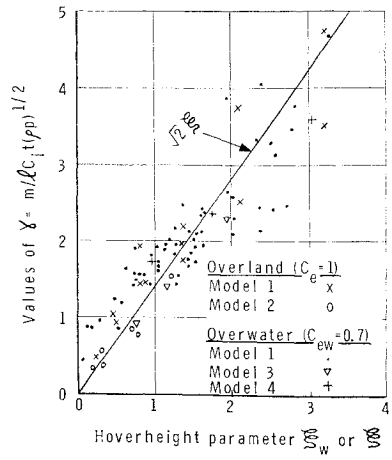

Fig. 2 Graphs of $\gamma = m/lC_i t(\rho p)^{1/2}$ vs ξ_w for overwater operation or ξ for overland operation.

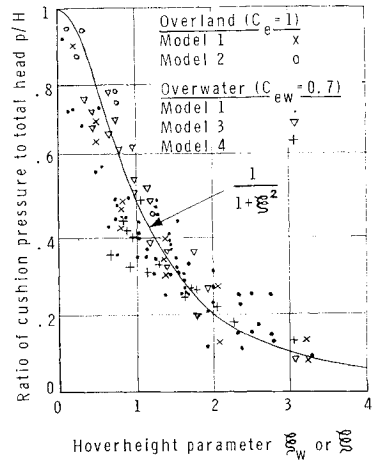

Fig. 3 Graphs of p/H against ξ_w for overwater operation or ξ for overland operation.

lower than 0.6 with simple orifices under any circumstances (see Ref. 4 for more detailed information).

If h is the height of the craft rim above the undisturbed water level, and Δh is the full depth of the depression caused by the discharging air (Fig. 4), then the parameter ξ defined as in the overland case becomes

$$\xi_w = C_{ew}(h + \Delta h)/C_i t \tag{4}$$

where the suffix w refers to the fact that this is for the over-water case.

The mass flow rate obtained from Eq. (1) is, therefore,

$$m/lC_i t(\rho p)^{1/2} = 2^{1/2}\xi_w \tag{5}$$

Now let J be the momentum of the air leaving the cushion, and ignore momentum losses in the discharge process; then, if V is the discharge velocity beyond the point of full contraction, Bernoulli's theorem gives

$$V = (2p/\rho)^{1/2} \tag{6}$$

and so

$$\begin{aligned} J = mV &= [lC_i t(\rho p)^{1/2} \times 2^{1/2}\xi_w](2p/\rho)^{1/2} \\ &= 2lC_i t\, p_{\xi w} \end{aligned} \tag{7}$$

In order to estimate Δh, now we consider the horizontal equilibrium of the water surface shown in Fig. 4,

$$\begin{aligned} p(p/w - \Delta h) + J(1 - \cos\phi) &= (w/2)\,(p/w)^2 l \\ \therefore\ \Delta h &= (p/2w) + J(1 - \cos\phi)/pl \end{aligned} \tag{8}$$

Let ϕ be the angle at which the air leaves the water surface; consider the vertical equilibrium at a point z in Fig. 4. The change in jet momentum in the vertical direction in a distance Δz is

$$J[dx/dz + (d^2x/dz^2)\Delta z] - J(dx/dz) = J(d^2x/dz^2)\Delta z$$

provided that the slope of the water surface is small. This must be equal to $\Delta z l w(\Delta h - x)$ for vertical equilibrium of the water surface, so that

$$d^2x/dz^2 + (wl/J)x = (wl/J)\Delta h \tag{9}$$

The only solution of this equation, which also satisfies the conditions $x = dx/dz = 0$ at $z = 0$, is

$$x = \Delta h\{1 - \cos[(wl/J)^{1/2}z]\} \tag{10}$$

But $x = \Delta h$ at $z = Z$, so that $\cos[(wl/J)^{1/2}Z] = 0$, and $\sin[(w/l/J)^{1/2}Z] = 1$. Finally, therefore,

$$\begin{aligned} \tan\phi = (dx/dz)_{z=Z} &= \Delta h(wl/J)^{1/2} \sin[(wl/J)^{1/2}Z] \\ &= \Delta h(wl/J)^{1/2} \end{aligned} \tag{11}$$

Using Eqs. (7) and (8), we now may write Eq. (11) in the form

$$\begin{aligned} \tan\phi &= \{(p/2w) + [J(1 - \cos\phi)]/lp\}(wl/J)^{1/2} \\ &= \Gamma^{1/2}\{1 + [(1 - \cos\phi)/2\Gamma]\} \end{aligned} \tag{12}$$

where

$$\Gamma = (1/8\xi_w)(p/wC_i t) \tag{13}$$

Equation (12) can be rewritten in the form of a quadratic equation for $\Gamma^{1/2}$ and solved to give

$$\Gamma^{1/2} = \tan\phi\{1 + [1 - (2\cos^2\phi)/(1 + \cos\phi)]^{1/2}\}/2 \tag{14}$$

Equation (14) must be evaluated numerically for ϕ in terms of Γ. The result is plotted as the curve labeled exact theory in Fig. 6. An approximate theory is developed in Appendix A which is slightly simpler, but leads to very much the same results. A comparison of the exact and approximate graphs of ϕ vs Γ is shown in Fig. 6. From Eqs. (8, 7, and 13) we now obtain $\Delta h/(p/w)$ in the form

$$\begin{aligned} \Delta h/(p/w) &= (\tfrac{1}{2}) + (2lC_i tp\xi_w/pl)(1 - \cos\phi)(w/p) \\ &= (\tfrac{1}{2})[1 + (1 - \cos\phi)/2\Gamma] \end{aligned} \tag{15}$$

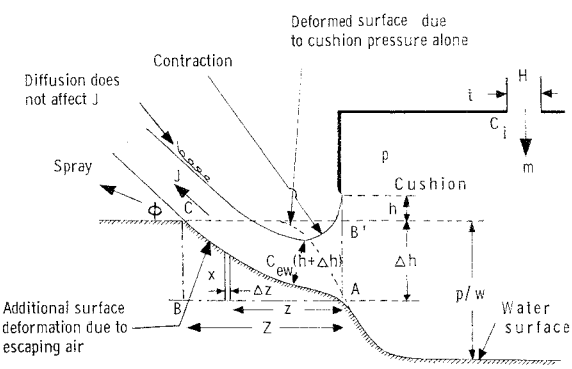

Fig. 4 Assumed path of air escaping from cushion.

Fig. 5 Photograph of model 3 showing deformed water surface.

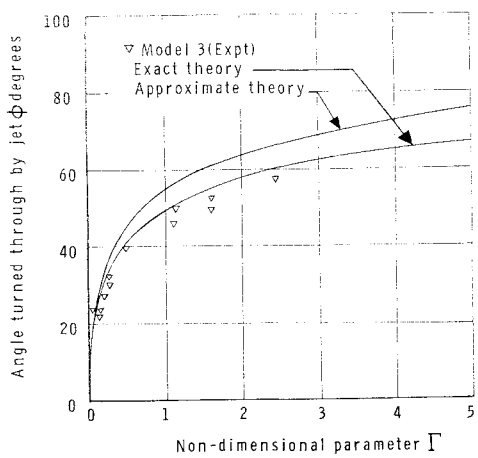

Fig. 6 Graphs of ϕ vs Γ for overwater operation.

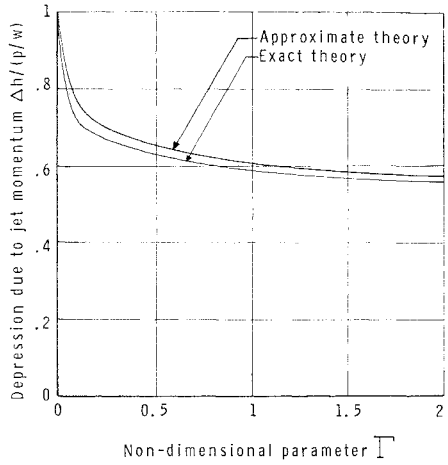

Fig. 7 Graphs of $\Delta h/(p/w)$ vs Γ for overwater operation.

The graphs of $\Delta h/(p/w)$ against Γ are plotted in Fig. 7 using the graph of ϕ vs Γ in Fig. 6. It is seen that

$$\Delta h/(p/w) = 0.7 \tag{16}$$

to within about 20%, even for large values of Γ. The value of ξ_w now becomes

$$\begin{aligned} \xi_w &= (C_{ew}/C_i)(h/t + 0.7p/wt) \\ &= 0.70h/C_it + 0.50p/C_iwt \end{aligned} \tag{17}$$

if we assume that $C_{ew} = 0.70$. Once ξ_w is known, all other quantities of interest, such as p/H and m, can be found.

Discussion of the Experimental Investigations of Overland and Overwater Performance

The apparatus used in the tests comprised a small wooden box of section shown in Fig. 8. A total head tube was used to measure the total head H, and a static pressure tube was used to measure the cushion pressure p. No means was available for measuring the mass flow m. However, since the inlet was a carefully shaped nozzle, $C_i = 1$ and Bernoulli's theorem gives

$$\left.\begin{aligned} H &= p + (\rho/2)(m/\rho lt)^2 = p\{1 + (\tfrac{1}{2})[m/lt(\rho p)^{1/2}]^2\} \\ \gamma &= m/lt(\rho p)^{1/2} = [(H/p) - 1]^{1/2}2^{1/2} \\ &= 2^{1/2}[(1/f) - 1]^{1/2} \end{aligned}\right\} \tag{18}$$

where $f = p/H$. This expression was used to determine the mass flow in terms of the measured values of p and H. The mass flow measurements were not strictly available for comparison with the theory, therefore, but the good agreement with theory in Fig. 2 is at least encouraging, since Bernoulli's theorem for well shaped nozzles is known to be accurate. Four models of the general type shown in Fig. 8 were made,

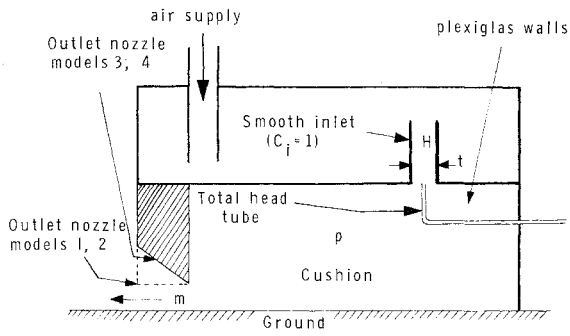

Fig. 8 Section of experimental equipment.

and the main dimensions are shown in Table 1. Some of the experimental data are given in Table 2. The term C_i was unity in all four cases. Figures 2 and 3 show the comparison between the experimental results and the theoretical expressions given in Eqs. (1) and (3), respectively, for the overland case. Only models 1 and 2 were used in the overland tests.

The height h of the rim edge of the plenum chamber model above the outside water level was varied over a wide range of values for models 1, 3, and 4, including some negative values. This is possible in the overwater case, since ξ_w still remains positive if Δh is sufficiently large. Some results of the tests are shown in Figs. 2 and 3, where the points obtained from the overland tests and the theoretical curves are superimposed. The agreement is seen to be encouraging. The scatter is undesirable, but seems to be inherent in overwater testing. This is partly because of difficulties of measurement but also because the interaction of the jet, the cushion, and the water surface is actually a complex hydrodynamic (and not merely hydrostatic) phenomenon. Considerable spray is generated, apparently increasing as Γ increases; and the water surface was observed at times to be in a state of violent oscillation. The analysis developed here is probably the simplest possible description of the phenomena involved; any more detailed analysis would have to take some account of the hydrodynamic aspects, also.

Prediction of the amount of spray generated is not yet possible. It will be seen (Fig. 9) that Z is very small when Γ is large, and (Fig. 6) that ϕ is large when Γ is large. Both of these factors are related, and show that violent turning of the escaping air occurs for large Γ. This reasonably can be expected to lead to large amounts of spray. On the other hand, when Γ is small, ϕ is small and Z is large, so that little spray can be expected. This reasoning leads one to suppose that a causal relationship may exist between the rate at which spray is generated and the value of Γ.

Values of the rate of spray generation were measured in some of the experiments, using a suitable vessel. A graph of $(h + \Delta h)M$ was first plotted against the cushion pressure p, where M is the mass of spray collected per unit time and $h + \Delta h$ is obtained from Eq. (17) using experimental values of p. The points were found to lie close to a curve of the type $p^{3/2}$, and the graph of $(h + \Delta h)M$ against $p^{3/2}$ then was drawn and shown to be a straight line, as in Fig. 10. Therefore,

$$\begin{aligned} (h + \Delta h)M &\propto p^{3/2} \\ M &\propto p^{3/2}/(h + \Delta h) \\ &\propto \Gamma p^{1/2} \end{aligned}$$

using Eq. (13) for Γ. We therefore see that

$$M/l(\rho p)^{1/2} \propto \Gamma \tag{19}$$

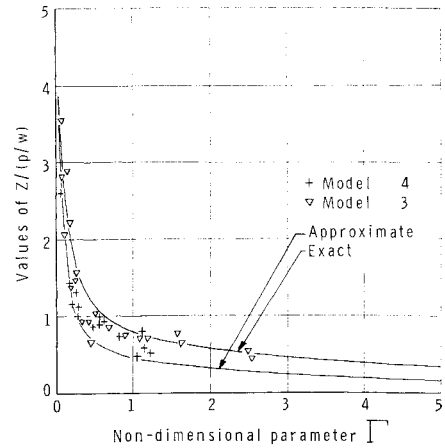

Fig. 9 Graphs of $Z/(p/w)$ vs Γ for overwater operation.

Table 1 Significant dimensions of test equipment

Model no.	1	2	3	4
Inlet thickness t, in.	0.31	0.91	0.48	0.31
Breadth, in.	2.0	3.80	3.25	3.13
Inlet discharge Coefficient C_i	1.0	1.0	1.0	1.0
Assumed discharge Coefficient C_e	1.00	1.00	...	...
Assumed discharge Coefficient C_{ew}	0.70	...	0.70	0.70

since M is obviously proportional to l for a two-dimensional model. A graph of $M/l(\rho p)^{1/2}$ is plotted vs Γ in Fig. 11. It is seen to be a straight line. Needless to say, further tests for other values of t are required before Eq. (19) definitely can be established. Certainly, the results for $t = 0.48$ in. and $t = 0.31$ in. fall on the same lines in Figs. 10 and 11.

A further point of interest is seen in Fig. 10, where the value of $(h + \Delta h)M$, although varying substantially in proportion to $p^{3/2}$, seems to approach zero for a small but nevertheless finite value of p. This is physically realistic, since low velocity jets (exit velocity is proportional to $p^{1/2}$) require a certain amount of momentum before surface tension can be overcome and spray droplets produced. The value of p at the spray cutoff point seems to be about 2 psf, but this may be a consequence of the scale of the model; further work on larger and better instrumented test facilities would be needed to study the problem in more detail. It is hoped that this paper will stimulate such an investigation.

Conclusions

A theory has been developed which relates the static behavior of a two-dimensional plenum chamber GEM over water to the geometrical characteristics and the total head of the air supply. In fact, a single nondimensional parameter is shown to control several observable phenomena. The experimental data is shown to support the theory. Experiments are also described in which the rate of spray generation was measured. It is shown that there is some evidence to support the view that a certain spray rate parameter depends only on the nondimensional parameter referred to previously. Suggestions for further work are made.

Appendix A: Alternative Solution for Overwater Performance

A simpler approach is of some interest. In this case, the path of the escaping air from A to C in Fig. 4 is assumed to be a straight line of angle ϕ to the horizontal, and the change in vertical momentum occurring suddenly at the point A is assumed to support the prism of fluid that would otherwise occupy the space $AB'C$. From the geometry, therefore,

$$Z = \Delta h \cot\phi \tag{A1}$$

Newton's second law, applied to equilibrium in the vertical direction, therefore gives

$$J \sin\phi = w\Delta h Z l/2 \tag{A2}$$

$$= (wl/2)(p/2w)^2[1 + 2wJ(1 - \cos\phi)/lp^2]^2 \cot\phi$$

using Eqs. (A1, 7, and 13). Equation (A2) may be written

$$(1 - \cos^2\phi)/\cos\phi = (\Gamma/2)[1 + (1 - \cos\phi)/2\Gamma]^2 \tag{A3}$$

and Eq. (A3) may be solved for Γ to give

$$\Gamma = [(1 - \cos\phi)/2\cos\phi][2 - \cos\phi + 2(1 - \cos\phi)^{1/2}] \tag{A4}$$

This particular graph of ϕ vs Γ is plotted in Fig. 6 and labeled the approximate theory.

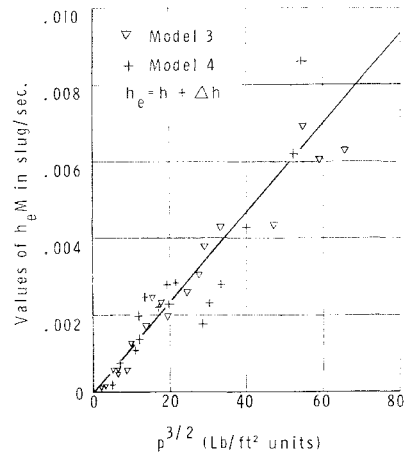

Fig. 10 Effect of cushion pressure p and hoverheight $h + \Delta h$ on the rate of spray generation M.

Appendix B: Shape of Deformed Water Surface

From Eq. (10) we see that

$$x/\Delta h = 1 - \cos[(wl/J)^{1/2}Z(z/Z)] = 1 - \cos(\pi z/2Z) \tag{B1}$$

Table 2 Some typical test measurements

Model no.	3	3	3	3	4	4
h, in.	+1.00	0.0	−0.50	−2.00	1.0	0.0
H, in. of water	1.63	2.25	2.00	4.12	3.75	4.10
p, in. of water	0.45	1.12	1.40	3.12	0.50	1.10
Z, in.	1.60	1.60	1.50	1.70	1.30	1.10
ϕ, deg	22	31	40	56	...	...
M, slug/sec ($\times 10^3$)	0.116	5.30	6.64	50.0	0.17	5.32
$0.7\,h/t$	1.46	0.0	−0.73	−2.91	22.4	0.0
$0.5\,p/wt$	0.47	1.16	1.46	3.24	0.80	1.77
$\xi_w = 0.7\,h/t + p/2wt$	1.93	1.16	0.73	0.33	3.04	1.77
$p/H = f$	0.277	0.5000	0.700	0.758	0.133	0.268
Γ	0.061	0.250	0.50	2.45	0.066	0.25
$Z/(p/w)$	3.56	1.46	1.07	0.55	2.60	1.00
$p^{3/2}$, psf	3.58	14.08	19.70	65.2	4.20	13.7
$(h + \Delta h)M = \xi_w tM$ slug-fps $\times 10^3$	0.084	2.45	1.93	6.28	0.14	2.44
$M/l\,(\rho p)^{1/2}$, ft	0.057	1.66	1.86	9.36	0.09	1.74
$\gamma = [2(1/f - 1)]^{1/2}$	2.29	1.41	0.93	0.80	3.61	2.34

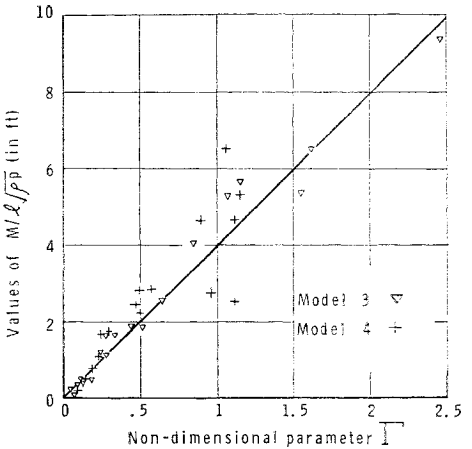

Fig. 11 Effect of parameter Γ on spray rate parameter.

using the fact that $\sin[(wl/J)^{1/2}Z] = 1$, or

$$(wl/J)^{1/2}Z = \pi/2$$

We also see from this equation and from Eq. (7) that

$$(wl)^{1/2}Z/(2lC_i tp\xi_w)^{1/2} = \pi/2$$

or

$$Z/(p/w) = \pi/4\Gamma^{1/2} \tag{B2}$$

using Eq. (13). The graph of $Z/(p/w)$ against Γ, corresponding to Eq. (B2), is plotted in Fig. 9. If the approximate theory of Appendix A is used, then Eq. (A1) gives

$$\begin{aligned} Z/(p/w) &= [\Delta h/(p/w)]\cot\phi \\ &= (\tfrac{1}{2})[1 + (1 - \cos\phi)/2\Gamma]\cot\phi \end{aligned} \tag{B3}$$

using Eq. (15). Using the relationship between ϕ and Γ obtained from Eq. (A4), we may evaluate $Z/(p/w)$ as a function of Γ. The values of $Z/(p/w)$ obtained from Eq. (B3) and (A4) are plotted in Fig. 9.

References

[1] Chaplin, H. R., "Ground effect machine research and development in the United States," David Taylor Model Basin Rept. 944 (1960).

[2] Eames, M. C., "Fundamentals of the stability and control of peripheral jet vehicles," Report, Pneumodynamics Corp., Bethesda, Md. (1960).

[3] Poisson-Quinton, P. and Bevert, A., "The principle and applications of ground effect vehicles," Bull. Assoc. Tech. Maritime Aeronaut. 60, 61–89 (1960).

[4] Henry, J. P., "Design of power plant installations-pressure loss characteristics of duct components," NACA Aeronautical Research Rept. L4–F26 (1944).